would be important for the two types of residue. It is hoped that higher resolution data for the Con A structure analyzed by molecular graphics methods may resolve these factors better.

In conclusion, the experimental approach described allows description of the properties of individual tyrosine and histidine residues, and potentially cysteine residues, in proteins. This should make possible studies of the roles of these residues in interaction sites and contribute to understanding how protein structure can affect the properties of individual residues.

ACKNOWLEDGMENTS

We thank Dr. M. Yaguchi for the amino acid analysis, Dr. H. Kaplan for helpful discussions, and K. Pepperdine for technical assistance.

Registry No. Con A, 11028-71-0; Dnp-F, 70-34-8; histidine, 71-00-1; tyrosine, 60-18-4.

REFERENCES

Agrawal, B. B. L., & Goldstein, I. J. (1967) *Biochim. Biophys. Acta 147*, 262–271.

Bosshard, H. R. (1979) *Methods Biochem. Anal. 25*, 273–301.

Carrington, D. M., Auffret, A., & Hanke, D. E. (1985) *Nature (London) 313*, 64–67.

Carver, J. P., Barber, B. H., & Fuhr, B. J. (1977) *Biochemistry 16*, 3141–3146.

Cockle, S. A., Kaplan, H., Hefford, M. A., & Young, N. M. (1982) *Anal. Biochem. 125*, 210–216.

Cunningham, B. A., Wang, J. L., Waxdal, M. J., & Edelman, G. M. (1975) *J. Biol. Chem. 250*, 1503–1512.

Hardman, K. D. (1979) in *Carbohydrate-Protein Interaction* (Goldstein, I. J., Ed.) pp 12–26, American Chemical Society, Washington, DC.

Hardman, K. D., Agarwal, R. C., & Freiser, M. J. (1982) *J. Mol. Biol. 157*, 69–86.

Kaplan, H., Stevenson, K. J., & Hartley, B. S. (1971) *Biochem. J. 124*, 284–289.

Kaplan, H., Long, B. G., & Young, N. M. (1980) *Biochemistry 19*, 2821–2827.

McCubbin, W. D., Oikawa, K., & Kay, C. M. (1971) *Biochem. Biophys. Res. Commun. 43*, 666–674.

McKenzie, G. H., Sawyer, W. H., & Nichol, L. W. (1972) *Biochim. Biophys. Acta 263*, 283–293.

Pflumm, M. N., & Beychok, S. (1974) *Biochemistry 13*, 4982–4987.

Reeke, G. N., Becker, J. W., & Edelman, G. M. (1975) *J. Biol. Chem. 250*, 1525–1547.

Rieder, R., & Bosshard, H. R. (1980) *J. Biol. Chem. 253*, 4732–4739.

Young, N. M. (1983) *FEBS Lett. 161*, 247–250.

Young, N. M., & Leon, M. A. (1974) *Biochim. Biophys. Acta 336*, 46–52.

Reassociation of Dimeric Cytoplasmic Malate Dehydrogenase Is Determined by Slow and Very Slow Folding Reactions†

Rainer Rudolph, Ingrid Fuchs, and Rainer Jaenicke*

Institut für Biophysik und Physikalische Biochemie, Universität Regensburg, D-8400 Regensburg, West Germany

Received June 4, 1985; Revised Manuscript Received October 31, 1985

ABSTRACT: Malate dehydrogenase occurs in virtually all eucaryotic cells in mitochondrial and cytoplasmic forms, both of which are composed of two identical subunits. The reactivation of the mitochondrial isoenzyme has been the subject of previous studies [Jaenicke, R., Rudolph, R., & Heider, I. (1979) *Biochemistry 18*, 1217–1223]. In the present study, the reconstitution of cytoplasmic malate dehydrogenase from porcine heart after denaturation by guanidine hydrochloride has been determined. The enzyme is denatured by >1.2 M guanidine hydrochloride; upon reconstitution, ~60% of the initial native enzyme can be recovered. The kinetics of reconstitution after maximum unfolding by 6 M guanidine hydrochloride were analyzed by fluorescence, far-ultraviolet circular dichroism, chemical cross-linking with glutaraldehyde, and activity measurements. After fast folding into structured intermediates (<1 min), formation of native enzyme is governed by two parallel slow and very slow first-order folding reactions ($k_1 = 1.3 \times 10^{-3}$ s^{-1} and $k_2 = 7 \times 10^{-5}$ s^{-1} at 20 °C). The rate constant of the association step following the slow folding reaction (determined by k_1) must be $>10^6$ M^{-1} s^{-1}. The energy of activation of the slow folding step is of the order of 9 ± 1 kcal/mol; the apparent rate constant of the parallel very slow folding reaction is virtually temperature independent. The intermediates of reassociation must be enzymatically inactive, since reactivation strictly parallels the formation of native dimers. Upon acid dissociation (pH 2.3), ~35% of the native helicity is preserved, as determined by circular dichroism. Despite the residual structure, reconstitution after short-term acid dissociation (5 min) is governed by the same slow and very slow folding reactions as those observed after unfolding by guanidine hydrochloride. After long-term acid incubation (24 h), both the rate and yield of reactivation decrease, presumably due to a conformational rearrangement within the acid-dissociated monomers.

The mechanism of folding of small monomeric proteins such as bovine pancreatic trypsin inhibitor or ribonuclease has been investigated in considerable detail [cf. Kim & Baldwin (1982)]. In the case of larger multidomain or oligomeric proteins, the acquisition of the native three-dimensional structure is more complex since chain folding, domain pairing, and subunit association need to be properly coordinated (Jaenicke, 1984). As a consequence, the yield of reconstitution is generally below

† This work was supported by grants from the Deutsche Forschungsgemeinschaft and the Fonds der Chemischen Industrie.

* Address correspondence to this author at Biochemie II, Universität Regensburg.

0006-2960/86/0425-1662$01.50/0

100%, and the conditions of denaturation and reassociation have to be optimized with respect to temperature, protein concentration, and solvent composition (Jaenicke & Rudolph, 1986).

Mechanistic studies concerning the pathway of reconstitution of oligomeric enzymes have been performed with several oligomeric dehydrogenases (Jaenicke & Rudolph, 1983). In this context, the tetrameric lactate dehydrogenases from porcine heart and skeletal muscle have been characterized most extensively. For both enzymes, association to dimers is fast, while tetramer formation is governed by a slow, rate-determining association step.

From a structural point of view, the dimeric mitochondrial and cytoplasmic isoenzymes of malate dehydrogenase are highly homologous with lactate dehydrogenase (Birktoft et al., 1982; Roderick & Banaszak, 1983). Reconstitution of mitochondrial malate dehydrogenase has been shown to be governed by slow folding, followed by dimer formation with a rate slower than the respective step in the case of lactate dehydrogenase by several orders of magnitude (Jaenicke et al., 1979). As indicated by earlier preliminary experiments, the cytoplasmic isoenzyme exhibits a totally different reconstitution pattern (Jaenicke & Rudolph, 1983).

In the present study, a detailed account of the mechanism of refolding, reassociation, and reactivation of cytoplasmic malate dehydrogenase is given. Upon reconstitution, structured intermediates are formed in a rapid reaction. Subsequent rearrangement of these intermediates in two parallel slow and very slow first-order folding reactions is rate determining. The association to the native dimer is very fast, with a rate of the order of a diffusion-controlled process.

Materials and Methods

Porcine supernatant or cytoplasmic malate dehydrogenase (s-MDH)[1] (EC 1.1.1.37), obtained from Sigma (St. Louis, MO), was further purified by affinity chromatography using Procion green H-E 4 BD (ICI, Organic Division, London) coupled to Sepharose 4B (Neben, 1979). Gdn·HCl (ultrapure) was purchased from Schwarz/Mann (Orangeburg, NY), glutaraldehyde (purissimum, 25% aqueous solution) from Fluka (Basel), and NADH from Boehringer Mannheim). Other reagents were of analytical grade.

The purified s-MDH had a specific activity of 550 IU/mg, as determined at 25 °C, pH 7.6, in the presence of 0.5 mM oxalacetate and 0.2 mM NADH. Enzyme concentrations were determined spectrophotometrically at 280 nm by using an extinction coefficient of $E_{1\,cm}^{0.1\%} = 1.08$ (Frieden et al., 1978). Molar concentrations refer to a subunit molecular weight of 35000. The enzyme was stored as a precipitate in the presence of 3.2 M $(NH_4)_2SO_4$.

Denaturation and dissociation were generally performed by 1-h incubation at 20 °C in 6 M Gdn·HCl, pH 7.6, either in 0.1 M sodium phosphate or in 0.2 M potassium phosphate. Acid dissociation of the enzyme was achieved by 5-min or 24-h incubation in 1 M glycine/H_3PO_4, pH 2.3. Renaturation and reassociation were initiated by appropriate dilution either with 0.1 M sodium phosphate, pH 7.6, or with 0.2 M potassium phosphate, pH 7.6. Reconstition data obtained in both buffer systems essentially gave the same results. Except for the cross-linking experiments, which were performed in the absence of dithioerythritol, all buffer solutions contained 1 or 10 mM EDTA and 1 or 10 mM dithioerythritol.

[1] Abbreviations: s-MDH, porcine supernatant or cytoplasmic malate dehydrogenase (EC 1.1.1.37); EDTA, (ethylenedinitrilo)tetraacetic acid; Gdn·HCl, guanidine hydrochloride; U, M*, and M, unfolded, partially folded, and folded monomers, respectively (parentheses indicate unstable intermediates which are not populated); D* and D, presumably dimeric intermediates and native dimers, respectively; k_1 and k_2, apparent first-order rate constants of the slow and very slow folding reactions, respectively; A_1 and A_2, relative amplitudes of the slow and very slow folding reactions, respectively; $NaDodSO_4$, sodium dodecyl sulfate.

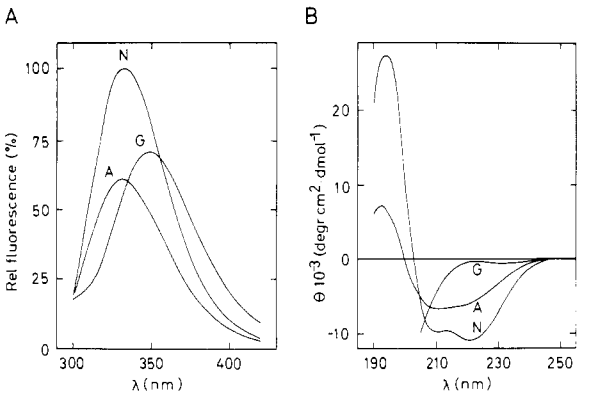

FIGURE 1: Spectral properties of native and denatured porcine s-MDH. (N) Native enzyme in 0.1 M sodium phosphate, pH 7.6; (A) acid-denatured enzyme in 1 M glycine/H_3PO_4, pH 2.3; and (G) s-MDH denatured by 6 M Gdn·HCl in 0.1 M sodium phosphate, pH 7.6; all solutions contained 1 mM EDTA. (A) Protein fluorescence: excitation wavelength 280 nm; protein concentration 12.5 μg/mL. (B) Far-UV circular dichroism: protein concentration 1.0 mg/mL; calculated for a mean residue molecular mass of 109.

Activity regain was determined by sampling aliquots of the reconstituting enzyme. The final yield of reactivation was determined after up to ~170 h, relative to a nondenatured sample kept under otherwise identical solvent conditions. The relative reactivation data are calculated relative to the final yield.

Reassociation was determined by using the glutaraldehyde cross-linking method (Hermann et al., 1981; Zettlmeissl et al., 1982a). Cross-linking was performed at 20 °C by 2-min incubation in the presence of 1.2% (w/v) glutaraldehyde. Under these conditions, ~90% cross-linking of the native dimer is obtained. The reassociation data are corrected accordingly to account for the incomplete fixation. To exclude perturbation of the cross-linking data by incomplete fixation of intermediates of reconstitution or by intermolecular cross-bridges, varying amounts of glutaraldehyde were applied. Identical results were obtained after fixation with 0.07–4.2% glutaraldehyde, which strongly suggests that the actual particle distribution of the reassociating enzyme is stabilized in the correct way. Cross-linking by glutaraldehyde and separation of the cross-linking products by $NaDodSO_4$–polyacrylamide slab gel electrophoresis were performed as described elsewhere (Hermann et al., 1981; Zettlmeissl et al., 1982a). Protein fluorescence was measured in a Perkin-Elmer MPF 44A spectrophotometer equipped with a Corrected Spectra accessory using native enzyme as the fluorescence standard. Circular dichroism was determined in a JASCO T-500A spectrophotometer equipped with a DP-500N data processor.

Results

Dissociation/Reassociation: Equilibrium Studies. Deactivation and denaturation of porcine s-MDH both by weak acid and by Gdn·HCl are accompanied by complete dissociation into the monomeric state, as confirmed by sedimentation analysis (R. Jaenicke, unpublished results).

The spectral properties (fluorescence, far-UV circular dichroism) reveal characteristic differences within the backbone structures after dissociation by weak acid (pH 2.3) on the one hand and 6 M Gdn·HCl on the other (Figure 1). Upon acid dissociation, the maximum of the intrinsic protein fluorescence remains unchanged (333 nm) although the fluorescence in-

Table I: Comparison of Native and Renatured Porcine s-MDH[a]

	native	reactivated
activity[b]		
A_{sp} (IU/mg)	550	542
$K_{M,oxac}$ (mM)	0.051	0.053
$K_{M,NADH}$	0.027	0.027
fluorescence emission		
maximum (nm)	333	333
intensity at 330 nm (%)	100	100
circular dichroism		
$\theta_{222\,nm}$ ($\times 10^{-3}$ deg·cm^2·dmol^{-1})	10.4	10.4
$\theta_{208\,nm}$ ($\times 10^{-3}$ deg·cm^2·dmol^{-1})	9.6	9.2
reactivation kinetics[c]		
yield (%)	51	51[d]
k_1 ($\times 10^3$ s^{-1})	1.7	1.2[d]
k_2 ($\times 10^5$ s^{-1})	9.0	5.2[d]
A_1 (%)	64	64[d]

[a] After denaturation/renaturation (cf. Figure 2) at a protein concentration of 10.5 μg/mL, the enzyme was concentrated by ultrafiltration and passed through a Sephadex G-100 superfine column (2.6 × 70 cm). [b] The value K_M for each substrate was determined at a constant concentration of the respective cosubstrate, i.e., 0.5 mM oxalacetate (oxac) or 0.2 mM NADH in 0.1 M sodium phosphate buffer, pH 7.6, containing 1 mM dithioerythritol and 1 mM EDTA at 25 °C. The numerical values were derived from Eadie–Hofstee or Lineweaver–Burk linearizations, which gave essentially the same results. [c] Rate constants of the slow and very slow steps of reactivation, k_1 and k_2, respectively, and relative amplitude of the slow step, A_1, upon renaturation (20 °C) at an enzyme concentration of 2.1 μg/mL after 1-h denaturation in 6 M Gdn·HCl. [d] Reactivated enzyme subjected to a second denaturation/renaturation cycle.

tensity at the given wavelength decreases by ~40%. Maximum unfolding of the dissociated subunits by 6 M Gdn·HCl results in a red shift of the emission maximum toward 350 nm (apart from a decrease in fluorescence intensity), which indicates the exposure of tryptophan side chains to the aqueous solvent (Teipel & Koshland, 1971). The far-UV circular dichroism of the native enzyme yields a helix content of 39% (Siegel et al., 1980). This figure agrees well with X-ray data, which show about 40% of the amino acid residues of s-MDH to be in helical conformations (Banaszak & Bradshaw, 1975). Upon acid dissociation, the helix content is reduced to 14%, while in the presence of 6 M Gdn·HCl the protein is essentially devoid of residual elements of secondary structure.

s-MDH can be deactivated by relatively low concentrations of Gdn·HCl (>1.2 M); apart from the incomplete reconstitution, the equilibrium transitions of deactivation and reactivation run closely parallel, with a transition midpoint at 0.6 M Gdn·HCl (data not shown).

Reactivation of the enzyme after complete unfolding by 6 M Gdn·HCl yields 60 ± 10% of the initial activity (average over all reactivation experiments). The reactivated enzyme is indistinguishable from native s-MDH with respect to the enzymatic and physicochemical properties summarized in Table I.

Refolding after Dissociation and Denaturation by Gdn·HCl. The refolding kinetics of s-MDH after unfolding by 6 M Gdn·HCl were monitored by protein fluorescence and far-UV circular dichroism. Immediately after dilution of the denaturant (<1 min), the wavelength of the fluorescence emission maximum is shifted back to the native value of 333 nm (Figure 2). The subsequent increase in protein fluorescence is determined by a slow first-order folding step, characterized by $k_1 = 1.3 \times 10^{-3}$ s^{-1} (20 °C). An additional very slow folding step (k_2) is detected if renaturation of s-MDH is analyzed by other spectroscopic or functional properties (see below); in fluorescence measurements, this reaction may either show a very low amplitude or escape detection because of the restricted long-term stability.

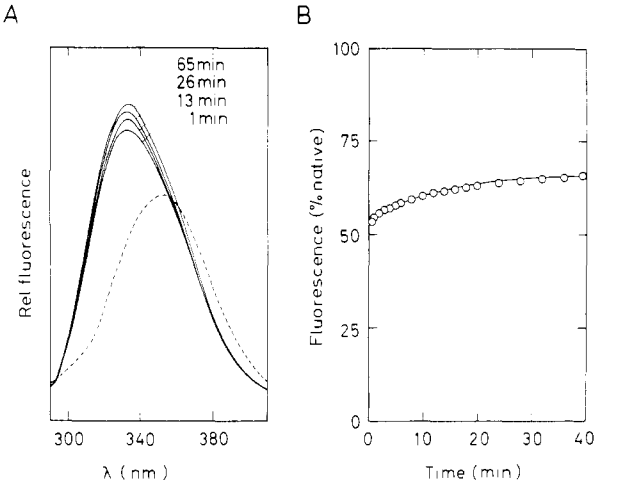

FIGURE 2: Refolding of s-MDH at 20 °C as determined by protein fluorescence after denaturation by 1-h incubation in 6 M Gdn·HCl. (A) Spectral changes during renaturation at an enzyme concentration of 16 μg/mL. Broken line, denatured s-MDH in 6 M Gdn·HCl; full line, renaturing enzyme at the given times of renaturation. (B) Kinetics of renaturation determined at an emission wavelength of 330 nm (λ_{ex} = 280 nm). The data points represent the average of five kinetic traces performed at a protein concentration of 21 μg/mL. 0% and 100% refer to the denatured and native fluorescence emission, respectively. The curve is calculated for a single first-order reaction with $k_1 = 1.3 \times 10^{-3}$ s^{-1}.

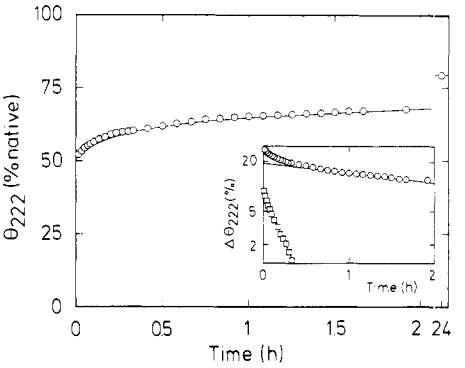

FIGURE 3: Kinetics of refolding of porcine s-MDH at 20 °C as determined by circular dichroism at 222 nm. Renaturation at an enzyme concentration of 20 μg/mL after 1-h denaturation by 6 M Gdn·HCl; 0% and 100% refer to denatured and native enzyme, respectively. The curve is calculated for two parallel first-order reactions with $k_1 = 1.3 \times 10^{-3}$ s^{-1} (relative amplitude 33%) and $k_2 = 7 \times 10^{-5}$ s^{-1} (relative amplitude 67%) for the slow and very slow phase, respectively. Insert: Determination of the rate constants resolved as the sum of two exponentials according to standard procedures (Frost & Pearson, 1961).

Recovery of the native secondary structure, as determined by far-UV circular dichroism, exhibits a multistep kinetic profile. Approximately 64% of the final ellipticity at 222 nm is regained in an initial fast reaction (<1 min) (Figure 3). The remaining 36% of the backbone structure is recovered by two further reactions: the slow folding step previously detected by fluorescence ($k_1 = 1.3 \times 10^{-3}$ s^{-1}, relative amplitude ~33%, 20 °C) and an additional very slow folding reaction ($k_2 = 6.9 \times 10^{-5}$ s^{-1}, relative amplitude ~67%).

Both fluorescence and circular dichroism show that structured intermediates are formed in a rapid reaction; native enzyme appears only after two subsequent slow isomerization reactions of these intermediates. On the basis of the spectroscopic data, it cannot be decided whether the two slow processes reflect a parallel or a consecutive reaction mechanism or whether the slow steps occur before or after dimer formation. Discrimination between these alternatives is rendered

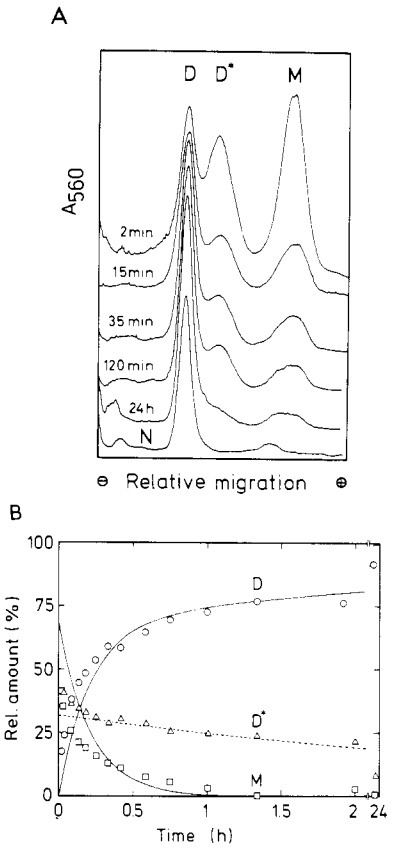

FIGURE 4: Kinetics of reassociation of s-MDH at 20 °C as determined by cross-linking. Reassociation at an enzyme concentration of 6.5 μg/mL after 1-h denaturation by 6 M Gdn·HCl. "Snap-shot analysis" of reassociation by 2-min cross-linking in the presence of 1.2% (w/v) glutaraldehyde and subsequent separation of the intermediates of association by slab gel electrophoresis. N, M, D, and D* stand for the native enzyme, monomers, dimers, and a (persumably dimeric) intermediate, respectively. (A) Band pattern of the products of cross-linking obtained after the given times of reassociation. Scans are given in arbitrary units. (B) Kinetics of reassociation as determined from the peak areas given in (A). Lines are calculated for two parallel first-order reactions with $k_1 = 1.3 \times 10^{-3}$ s^{-1} for the slow phase (relative amplitude 68%) and $k_2 = 7 \times 10^{-5}$ s^{-1} for the very slow phase (relative amplitude 32%).

possible by determining the time course of reassociation directly by means of cross-linking techniques.

Reassociation after Dissociation and Denaturation by Gdn·HCl. The kinetics of reassociation of oligomeric proteins can be analyzed by fast chemical cross-linking with glutaraldehyde (Hermann et al., 1981, 1983a; Zettlmeissl et al., 1982a). Subsequent analysis of the cross-linked material by NaDodSO$_4$–polyacrylamide gel electrophoresis allows determination of the rate constants of individual association steps as well as identification of intermediates of association.

As shown in Figure 4, in the case of s-MDH, part of the monomers (~32%) rapidly form a presumably dimeric intermediate which is characterized by a slightly higher electrophoretic mobility, in comparison with cross-linked native dimers. These intermediates are transformed into dimers with native migration properties by the very slow folding step (k_2), previously identified by circular dichroism (cf. Figure 3). The remaining monomers (68%) form native dimers in a parallel reaction, the rate of which is determined by the slow folding step (k_1).

Reactivation after Dissociation and Denaturation by Gdn·HCl. The kinetics of reactivation of porcine s-MDH after complete deactivation are determined by the same parallel slow folding reactions previously determined for renaturation and

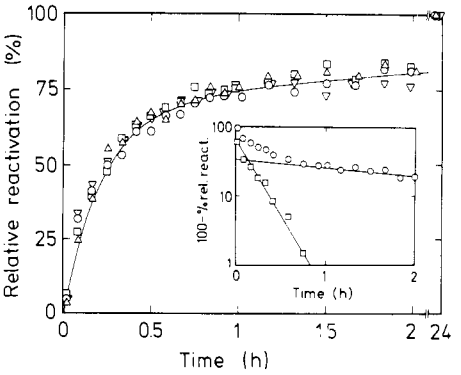

FIGURE 5: Kinetics of reactivation of s-MDH at 20 °C after 1-h denaturation by 6 M Gdn·HCl. Reactivation at varying enzyme concentrations (micrograms per milliliter): 1.3 (○); 3.7 (△); 6.4 (□); and 12.9 (▽). Reactivation starts from zero activity. It is calculated relative to the final yield of 51 ± 12% of the initial activity, as determined after up to 172 h of reconstitution. The solid line is calculated according to two parallel first-order reactions with $k_1 = 1.3 \times 10^{-3}$ s^{-1} for the slow phase (relative amplitude 68%) and $k_2 = 7 \times 10^{-5}$ s^{-1} for the very slow phase (relative amplitude 32%). Insert: Determination of the rate constants resolved as the sum of two exponentials for a representative reactivation experiment at an enzyme concentration of 1.3 μg/mL.

Table II: Effect of Enzyme Concentration on Slow and Very Slow Steps of Reactivation of Porcine s-MDH after 1-h Denaturation in 6 M Gdn·HCl[a]

protein concn (μg/mL)	temp (°C)	k_1 (×10^3 s^{-1})[b]	k_2 (×10^5 s^{-1})[c]	A_1[d] (%)
12.4	0	0.36	4.5	54
6.2	0	0.37	2.7	51
2.5	0	0.34	3.3	53
12.9	20	1.4	5.3	68
6.4	20	1.5	8.7	67
3.7	20	1.2	6.8	69
3.5	20	1.5	9.0	69
3.2	20	1.2	4.9	70
2.6	20	1.0	5.5	67
1.3	20	1.4	9.1	65

[a] The two rate constants were derived as the sum of two exponentials as described in Figure 3, insert. [b] Rate constants of the slow step. [c] Rate constant of the very slow step. [d] Relative amplitude of the slow step.

Table III: Effect of Time of Denaturation by Gdn·HCl on Kinetics of Reactivation of Porcine s-MDH[a]

denaturation				
time	temp (°C)	k_1 (×10^3 s^{-1})	k_2 (×10^5 s^{-1})	A_1 (%)
5 s	0	1.2	8.5	70
10 s	0	1.2	7.4	72
30 s	20	1.6	3.0	70
2 min	0	1.3	7.3	73
5 min	20	1.2	6.2	67
10 min	0	1.3	6.6	75
1 h	20	1.2	4.3	70
24 h	20	1.0	3.7	57

[a] Reactivation at 20 °C at an enzyme concentration of 4 ± 0.4 μg/mL. The final yield, determined after up to 144 h, was 71 ± 10% of the initial activity.

reassociation; at zero time (immediately after dilution), reactivation starts from zero activity. The relative amplitudes of the two kinetic phases are those obtained by chemical cross-linking (Figure 5). The rate of reactivation does not depend on enzyme concentration in the range from 1.3 to 13 μg/mL, at both 0 and 20 °C (Table II). Similarly, essentially unchanged kinetics of reactivation are observed upon variation of the time of denaturation in 6 M Gdn·HCl between 5 s and 24 h (Table III). Furthermore, both the rate constants and

Table IV: Effect of Stabilizing and Destabilizing Salt on Kinetics of Reactivation of Porcine s-MDH[a]

$[(NH_4)_2SO_4]$ (M)	[Gdn·HCl] (M)	k_1 ($\times 10^3$ s^{-1})	k_2 ($\times 10^5$ s^{-1})	A_1 (%)
present during reactivation[b]				
0	0.12	1.1	5.2	70
0.3	0.12	1.0	3.7	46
0.6	0.12	1.7	2.6	29
0.9	0.12	1.3	1.5	27
1.2	0.12	1.5	1.8	32
1.5	0.12	0.8	4.6	50
0	0.17	1.2	4.6	60
0	0.22	1.3	4.1	65
0	0.27	1.5	4.8	64
0	0.32	1.1	2.4	65
0	0.42	1.2	5.3	58
present in the enzyme assay[c]				
0	0	1.6	4.5	76
1.0	0	1.0	8.1	70
1.5	0	1.7	8.0	70
0	0.32	1.1	4.1	60

[a] Deactivation at 20 °C by 1-h incubation in 6 M Gdn·HCl; reactivation at 20 °C with the given amount of $(NH_4)_2SO_4$ or Gdn·HCl, present either during reactivation or in the enzyme assay. Enzyme concentration during reactivation was 4 ± 0.4 μg/mL. The final yield of reactivation, determined after up to 168 h, was found to decrease in the presence of $(NH_4)_2SO_4$ during reactivation. Otherwise the final yield was 64 ± 4% of the initial activity. [b] Activity measured under standard test conditions. [c] Reactivation in the presence of 0.12–0.32 M residual Gdn·HCl concentration.

Table V: Effect of Temperature on Rates of the Faster and Slower Steps of Reactivation of Porcine s-MDH[a]

temp (°C)	k_1 ($\times 10^3$ s^{-1})	k_2 ($\times 10^5$ s^{-1})	A_1 (%)
0	0.4	4.8	42
5	0.6	4.4	53
10	0.7	3.3	62
15	0.8	4.0	65
25	1.6	2.7	75
30	1.9	3.0	80
35	2.2	2.5	81

[a] Deactivation at 20 °C by 1-h incubation in 6 M Gdn·HCl, followed by thermal equilibration. Enzyme concentration during reactivation was 4.6 μg/mL; the final yield, determined after up to 168-h reactivation, was 72 ± 2% of the initial activity. From the given data, an energy of activation of 9 ± 1 kcal/mol for the slow step (k_1), and of essentially zero for the very slow step (k_2), is derived.

relative amplitudes of the two phases are not affected by the presence of up to 0.42 M Gdn·HCl during reactivation (Table IV). Addition of stabilizing salt $[(NH_4)_2SO_4]$, which has no significant effect on the rate constants, leads to a decrease of the yield of reactivation and to variation of the relative amplitudes of the two parallel reactions (Table IV). Adding stabilizing or destabilizing salt to the enzyme assay does not change the kinetics of reactivation (Table IV).

From the temperature dependence of the reactivation data, an energy of activation of 9 ± 1 kcal/mol was calculated for the slow kinetic phase (Table V). The apparent rate constant (k_2) of the very slow phase does not depend significantly on temperature, although the relative amplitude of this phase decreases from 58% at 0 °C to 19% at 35 °C (Table V).

Reactivation after Acid Dissociation. A considerable portion of the backbone structure of porcine s-MDH is preserved upon acid dissociation, as determined by circular dichroism (cf. Figure 1). When the reactivation kinetics after short-term acid dissociation (5 min at pH 2.3) and unfolding by 6 M Gdn·HCl are compared, the kinetic constants are found to be virtually identical (Table VI; cf. Table II). Obviously, the residual structure does not play a significant role in the rate-limiting steps of reactivation. Similarly, addition of

Table VI: Reactivation of Porcine s-MDH at Various Enzyme Concentrations after Short-Term Acid Denaturation[a]

protein concn (μg/mL)	k_1 ($\times 10^3$ s^{-1})	k_2 ($\times 10^5$ s^{-1})	A_1 (%)
5.3	1.7	6.5	77
2.6	1.4	5.5	77
1.3	1.8	6.0	83
0.53	1.5	3.2	67
0.26	1.4	4.0	70
0.13	1.3	3.3	69

[a] Dissociation by 5-min incubation at 20 °C in 1 M glycine/H_3PO_4, pH 2.3, containing 1 mM dithioerythritol and 1 mM EDTA. Reactivation at 20 °C in 0.2 M potassium phosphate, pH 7.6, containing 10 mM dithioerythritol and 10 mM EDTA. The rate constants and amplitudes of the slow and very slow phases were derived as illustrated in Figure 4, insert. The final yield of reactivation, which amounts to 40 ± 6%, was determined after up to 336 h of reactivation. Reactivation in the presence of 10 mM NAD^+ does not yield significant alterations of the kinetic data: $k_1 = (1.33 \pm 0.25) \times 10^{-3}$ s^{-1}, $k_2 = (4.8 \pm 1.7) \times 10^{-5}$ s^{-1}, and $A_1 = 69 \pm 4\%$ for the given range of protein concentrations.

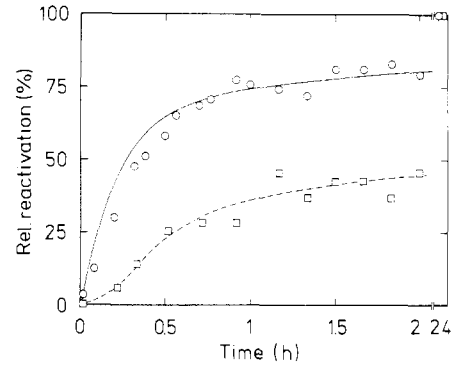

FIGURE 6: Effect of additional Gdn·HCl denaturation on the kinetics of reactivation of porcine s-MDH after long-term acid dissociation. Dissociation by 24-h incubation at 20 °C in 1 M glycine/H_3PO_4, pH 2.3, plus 1 mM dithioerythritol and 1 mM EDTA. Reactivation in 0.2 M potassium phosphate, pH 7.6, plus 10 mM dithioerythritol and 10 mM EDTA with (○) and without (□) a further denaturation step (2.5 min) in 6 M Gdn·HCl prior to reactivation. Reactivation starts from zero activity. After acid plus guanidine denaturation, the kinetics of reactivation may be calculated with the parameters given in Figure 4 (full line), and the final yield of reactivation increases from 28% to 45%.

NAD^+ during reactivation has no effect on the yield, rate, and relative amplitudes of the slow folding steps (Table VI).

Upon long-term acid dissociation, both the rate and yield of reactivation decrease, and the kinetics become increasingly sigmoidal (Figure 6). A similar effect previously observed in the case of tetrameric porcine muscle lactate dehydrogenase was explained by slow conformational changes within the partially structured subunits (Zettlmeissl et al., 1981, 1983). Obviously, upon long-term acid dissociation, the monomers become trapped in a "wrong" structure, from which refolding proceeds more slowly and with a low yield. In the present case, a similar mechanism seems to be operative, since the acid effect may be completely eliminated by additional unfolding, e.g., by 6 M Gdn·HCl.

Discussion

Reconstitution of oligomeric proteins after dissociation and denaturation requires proper coordination of the individual steps involved in the sequential mechanism of quaternary structure formation: folding of domains, merging of these "local structures", and formation of the correct subunit interfaces, followed by specific association to the functional assembly (Jaenicke, 1984). In many cases, the correct path-

way of folding and association is in kinetic competition with the formation of inactive byproducts (Zettlmeissl et al., 1979). Definition of denaturation/renaturation conditions which minimize the side reactions is of considerable technical importance, e.g., for the regeneration of enzyme reactors or for the activation of protein from "refractile bodies" frequently found in overproducing transformed microorganisms.

For reassociation studies, cytoplasmic and mitochondrial malate dehydrogenases from porcine heart represent a most simple model case, since only one association step is involved in the reconstitution of the homologous dimers. Reactivation of the mitochondrial isoenzyme after Gdn·HCl, urea, and acid dissociation has been previously reported to be determined by a slow folding step, followed by slow subunit association ($k_1 = 6.5 \times 10^{-4}$ s^{-1}, $k_2 = 3 \times 10^4$ M^{-1} s^{-1} at 20 °C; Jaenicke et al., 1979).[2]

A stringent kinetic analysis of reassociation requires that the protein does not change its quaternary structure upon varying protein concentration (Jaenicke & Rudolph, 1985). In the case of mitochondrial malate dehydrogenase, it has been reported that the enzyme at pH <7.5 undergoes concentration-dependent dissociation into the monomers (Bleile et al., 1977; Wood et al., 1978). However, under the conditions of our previous reconstitution experiments (pH 7.6), dissociation at low protein concentrations was not detectable (Jaenicke et al., 1979). As to the cytoplasmic isoenzyme from porcine heart, it is well established that the dimeric structure is preserved at low enzyme concentrations under a variety of solvent conditions (Bleile et al., 1977).

s-MDH is dissociated and unfolded by 6 M Gdn·HCl; far-UV circular dichroism as well as the red shift of protein fluorescence is indicative for the exposure of aromatic side chains at high denaturant concentration (Teipel & Koshland, 1971). Upon dissociation at acid pH (pH 2.3), the monomers retain part of their structure: the fluorescence maximum is not shifted to longer wavelengths, and the helix content (determined by far-UV circular dichroism) is only reduced to about one-third of the native value.

Except for the incomplete reconstitution, the equilibrium transitions of the Gdn·HCl-dependent deactivation and reactivation are superimposable in the case of s-MDH. Obviously, deactivation/reactivation is not perturbed by side reactions such as aggregation, in the transition range which has led to "hysteresis" in the case of several other oligomeric dehydrogenases (Jaenicke & Rudolph, 1983). The reconstituted enzyme amounts to ~60% of the starting material; it is a dimer indistinguishable from native s-MDH.

Incomplete reconstitution has been observed for most oligomeric enzymes. In the present case, it cannot be ascribed to heterogeneity of the starting material, since subsequent cycles of denaturation/renaturation result in a further lowering of recovery of activity (Table I); the fractional recovery equals 0.5^n, with n as the number of cycles.

The time-dependent recovery of the native structure after maximal unfolding by Gdn·HCl was monitored by spectroscopic, cross-linking, and activity measurements. Both fluorescence and far-UV circular dichroism prove structured intermediates to be formed within the time of manual mixing (<1 min). Immediately after native conditions are reestablished by diluting the denaturant, the ellipticity increases to ~64% of the final value. Regain of the complete native secondary structure is determined by two slow and very slow folding reactions ($k_1 = 1.3 \times 10^{-3}$ s^{-1}, $k_2 = 7 \times 10^{-5}$ s^{-1}, 20 °C: cf. Figure 1).

Fast formation of a compact globular structure ("molten globule" state) followed by slow reactivation and slow formation of the final tertiary structure has been previously reported for the renaturation of several monomeric and oligomeric proteins (Ohgushi & Wada, 1983; Jaenicke & Rudolph, 1983; Hermann et al., 1983a; Zettlmeissl et al., 1984).

A mechanistic interpretation of the kinetic data may be accomplished by fast chemical cross-linking (Hermann et al., 1979, 1981; Zettlmeissl et al., 1982a). Fixation of the intermediates of association of s-MDH with glutaraldehyde proves that for part of the polypeptide chains, formation of the native dimers is determined by a slow folding step at the monomer level, characterized by the same rate constant previously determined by spectroscopy ($k_1 = 1.3 \times 10^{-3}$ s^{-1}, relative amplitude ~68%, 20 °C). The remaining chains rapidly form a dimeric intermediate which is rearranged to the native dimer by very slow folding ($k_2 = 7 \times 10^{-5}$ s^{-1}, relative amplitude 32%, 20 °C). The differing migration properties of the "dimeric intermediate" and the native dimer upon $NaDodSO_4$ electrophoresis may be explained by a more extensive cross-linking of the native dimer: more compact molecules would bind less $NaDodSO_4$ and thus migrate more slowly in polyacrylamide gels than chains with fewer cross-links. A similar effect has been previously determined in cross-linking studies with aspartate transcarbamoylase (Burns & Schachman, 1982).

On the basis of the given data, folding and association of s-MDH may be described by the kinetic mechanism:

$$2(U) \xrightarrow{\text{fast}} 2M^* \xrightarrow{k_1} 2(M) \xrightarrow{\text{fast}} D \quad (68\% \text{ at } 20\ ^\circ\text{C})$$

$$2(U) \xrightarrow{\text{fast}} D^* \xrightarrow{k_2} D \quad (32\% \text{ at } 20\ ^\circ\text{C}) \qquad (1)$$

In this scheme, U, M*, and M stand for unfolded, partially folded, and folded monomers, respectively, D* for an incorrectly folded (presumably dimeric) intermediate, and D for the native dimer.

The formation of inactive material (as an additional competitive parallel reaction) is not considered in the present mechanism. Since the inactive material can be separated from native dimers by gel filtration, it must consist of high molecular weight aggregates. As in the case of lactate dehydrogenase, aggregate formation must be caused by kinetic competition with the fast formation of the previously mentioned compact globular structure (Rudolph & Jaenicke, 1986). This side reaction does not interfere with the kinetic analysis of reactivation which only concerns active material. In the analysis of reassociation by cross-linking, the covalently stabilized aggregates may also be neglected as they do not penetrate the polyacrylamide gel. However, the side reaction may perturb the kinetic data obtained by spectroscopic techniques, provided that the spectral properties of the aggregates deviate from the denatured enzyme. In this case, the relative amplitude of the initial fast phase will be affected by aggregate formation.

The structural properties of the intermediates may be elucidated by comparison of the relative amplitudes of the respective phases of folding and association (Table VII). The data clearly show that the partially folded monomer M* is structured to a considerably higher degree than the incorrectly folded dimeric intermediate D*.

The regain of enzymatic function strictly parallels the formation of native dimers; it is governed by the same slow

[2] In a recent investigation, reassociation of mitochondrial malate dehydrogenase after dissociation at pH 5 has been described by first-order kinetics (Wood et al., 1981). This interpretation may be erroneous, since the rate constants given in this report were found to be dependent upon protein concentration.

Table VII: Structural and Functional Properties of Intermediates of Reassociation of Porcine s-MDH[a]

intermediate[b]	activity (%)[c]	θ_{222} (%)[c]	fluorescence[d] (%)[c]
U	0	0	0
M*	0	83	80
D*	0	24	nd[e]
D	100	100	100

[a] Comparison of the kinetics of renaturation, reassociation, and reactivation (cf. Figures 2–5). [b] Intermediates defined in eq 1. [c] 0% and 100% refer to the denatured and renatured enzyme, respectively. [d] Determined at 330 nm. [e] Not determined.

and very slow folding reactions. Obviously, the populated intermediates, M* and D*, must be inactive, at least under standard test conditions (Table VII).

For porcine muscle lactate dehydrogenase, intermediates of reassociation could be partially activated by adding stabilizing salt to the test mixture (Girg et al., 1983). In the present case, activity measurements in the presence of up to 1.5 M $(NH_4)_2SO_4$ did not result in the activation of the given intermediates of reactivation (cf. Table IV).

Reactivation of s-MDH does not depend on protein concentration in the range from 1.3 to 13 μg/mL. This means that the association step following the slow formation of (M) must be of the order of $\geq 10^6$ M^{-1} s^{-1}, i.e., in the range of a diffusion-controlled association (Gutfreund, 1972). Compared to other dimeric dehydrogenases, such as mitochondrial malate dehydrogenase (Jaenicke et al., 1979) or D-lactate dehydrogenase from *Limulus polyphemus* (Gerl et al., 1985), dimer formation of s-MDH is faster by 2 orders of magnitude at least.

Considering assembly reactions of related proteins, the formation of the dimeric intermediate of tetrameric lactate dehydrogenase from pig muscle is found to be governed by a similarly fast association step (Hermann et al., 1983b). All these systems are homologous with respect to sequence and structure and apparently share a common *Q* axis (Birktoft et al., 1983; Roderick & Banaszak, 1983). Obviously, the rates of association may vary within a wide range, despite the close similarity of the dehydrogenases.

Both mitochondrial and cytoplasmic malate dehydrogenases are synthesized on free polysomes as products of two different nuclear genes (Chien & Fasman, 1984). Hybrids of the two isoenzyme forms have not been detected either in vivo or in vitro (Kimball & Wolfe, 1977). It may be assumed that hybrid formation is prevented by the widely differing rates of subunit association.

An interesting aspect of the present investigation is the formation of native dimers in two parallel reactions. Chemically distinct subforms of the enzyme, as frequently observed in the case of malate dehydrogenases [cf. Banaszak & Bradshaw (1975)], may be excluded as cause for the biphasic kinetics, since no significant heterogeneity could be observed during native and $NaDodSO_4$ gel electrophoresis (data not shown). Similarly, the strong dependence of the relative amplitudes of both kinetic phases on the refolding temperature (without concomitant change in the yield of reactivation) strongly suggests that the parallel reactions are not induced by heterogeneity (cf. Table V).

Cis–trans isomerization reactions around X–Pro peptide bonds may be another reason for parallel folding reactions, as observed for several small monomeric proteins (Brandts et al., 1975; Kim & Baldwin, 1982). If proline isomerism accounts for the formation of native s-MDH via parallel folding reactions, the relative amplitudes of both phases should depend on the time of denaturation. Upon short-term denaturation at low temperature (e.g., 5 s at 0 °C), the X–Pro peptide bonds of the denatured chains should still be in the native isomeric form, and the faster phase should predominate upon refolding. As indicated by the independence of the reactivation kinetics of the time of denaturation, the parallel slow and very slow folding reactions must be determined by rate-limiting steps other than proline isomerism (Table III). A similar result has been previously obtained for the refolding of porcine muscle lactate dehydrogenase (Zettlmeissl et al., 1982b).

As previously discussed, the monomers of s-MDH retain a considerable part of their backbone structure upon acid dissociation. Despite that, the kinetics of reactivation are essentially indistinguishable after short-term acid dissociation or after maximal unfolding by Gdn·HCl. This clearly proves that both rate-determining steps are relatively late events on the reconstitution pathway. The decrease in both the rate and yield of reactivation observed after long-term acid incubation may be determined by rearrangements similar to those described previously for lactate dehydrogenase (Zettlmeissl et al., 1981).

ACKNOWLEDGMENTS

We thank Dr. Franz X. Schmid for fruitful discussions. We gratefully acknowledge the excellent technical assistance of Inge Strobel.

Registry No. MDH, 9001-64-3; oxac, 328-42-7; NADH, 58-68-4.

REFERENCES

Banaszak, L. J., & Bradshaw, R. A. (1975) *Enzymes, 3rd Ed. 11*, 369–396.

Birktoft, J. J., Fernley, R. T., Bradshaw, R. A., & Banaszak, L. J. (1982) *Proc. Natl. Acad. Sci. U.S.A. 79*, 6166–6170.

Bleile, D. M., Schulz, R. A., Harrison, J. H., & Gregory, E. M. (1977) *J. Biol. Chem. 252*, 755–758.

Brandts, J. F., Halvorson, H. R., & Brennan, M. (1975) *Biochemistry 14*, 4953–4963.

Burns, D. L., & Schachman, H. K. (1982) *J. Biol. Chem. 257*, 8638–8647.

Chien, S.-M., & Freeman, K. B. (1984) *J. Biol. Chem. 259*, 3337–3342.

Frieden, C., Honegger, J., & Gilbert, H. R. (1978) *J. Biol. Chem. 253*, 816–820.

Frost, A. A., & Pearson, R. G. (1961) *Kinetics and Mechanism*, 2nd ed., Wiley, New York, London, and Sidney.

Gerl, M., Rudolph, R., & Jaenicke, R. (1985) *Biol. Chem. Hoppe-Seyler 366*, 447–454.

Girg, R., Rudolph, R., & Jaenicke, R. (1983) *FEBS Lett. 163*, 132–135.

Gutfreund, H. (1972) in *Enzymes: Physical Principles*, p 159, Wiley, London.

Hermann, R., Rudolph, R., & Jaenicke, R. (1979) *Nature (London) 277*, 243–245.

Hermann, R., Jaenicke, R., & Rudolph, R. (1981) *Biochemistry 20*, 5195–5201.

Hermann, R., Rudolph, R., Jaenicke, R., Price, N. C., & Scobbie, A. (1983a) *J. Biol. Chem. 258*, 11014–11019.

Hermann, R., Jaenicke, R., & Kretsch, G. (1983b) *Naturwissenschaften 70*, 517–518.

Jaenicke, R. (1984) *Angew. Chem., Int. Ed. Engl. 23*, 395–413.

Jaenicke, R., & Rudolph, R. (1983) *Colloq. Ges. Biol. Chem. 34th*, 62–90.

Jaenicke, R., & Rudolph, R. (1986) *Methods Enzymol.* (in press).

Jaenicke, R., Rudolph, R., & Heider, I. (1979) *Biochemistry 18*, 1217–1223.

Kim, P. S., & Baldwin, R. L. (1982) *Annu. Rev. Biochem. 51*, 459–489.
Kimball, D. F., Wolfe, R. G. (1977) *Arch. Biochem. Biophys. 181*, 33–38.
Neben, J. (1979) *Thesis*, TU Braunschweig.
Ohgushi, M., & Wada, A. (1983) *FEBS Lett. 164*, 21–24.
Roderick, S. L., & Banaszak, L. J. (1983) *J. Biol. Chem. 258*, 11636–11642.
Siegel, J. B., Steinmetz, W. E., & Long, G. L. (1980) *Anal. Biochem. 104*, 160–167.
Teipel, J. W., & Koshland, D. E., Jr. (1971) *Biochemistry 10*, 798–805.
Wood, D. C., Hodges, C. T., & Harrison, J. H. (1978) *Biochem. Biophys. Res. Commun. 82*, 943–950.
Wood, D. C., Jurgensen, S. R., Geesin, J. C., & Harrison, J. H. (1981) *J. Biol. Chem. 256*, 2377–2382.
Zettlmeissl, G., Rudolph, R., & Jaenicke, R. (1979) *Biochemistry 18*, 5567–5571.
Zettlmeissl, G., Rudolph, R., & Jaenicke, R. (1981) *Eur. J. Biochem. 121*, 169–175.
Zettlmeissl, G., Rudolph, R., & Jaenicke, R. (1982a) *Biochemistry 21*, 3946–3950.
Zettlmeissl, G., Rudolph, R., & Jaenicke, R. (1982b) *Eur. J. Biochem. 125*, 605–608.
Zettlmeissl, G., Rudolph, R., & Jaenicke, R. (1983) *Arch. Biochem. Biophys. 224*, 161–168.
Zettlmeissl, G., Teschner, W., Rudolph, R., Jaenicke, R., & Gäde, G. (1984) *Eur. J. Biochem. 143*, 401–407.

Human High Molecular Weight Kininogen as a Thiol Proteinase Inhibitor: Presence of the Entire Inhibition Capacity in the Native Form of Heavy Chain†

Shigeki Higashiyama, Iwao Ohkubo,* Hiroshi Ishiguro, Mitoshi Kunimatsu, Kohei Sawaki, and Makoto Sasaki
Department of Biochemistry, Nagoya City University Medical School, Mizuho-ku, Nagoya 467, Japan
Received August 29, 1985

ABSTRACT: High molecular weight (HMW) kininogen was purified from fresh human plasma by two successive column chromatographies on DEAE-Sephadex A-50 and Zn-chelate Sepharose 4B. The purified HMW kininogen appeared to be a single band on sodium dodecyl sulfate (SDS)–polyacrylamide disc gel electrophoresis in both the presence and absence of β-mercaptoethanol. However, it gave two bands on nonreduced SDS–polyacrylamide slab gel electrophoresis, a major band of dimeric form (M_r 200 000, ca. 95%) and a minor band of monomeric form (M_r 105 000, ca. 5%). Under reduced conditions, the dimeric form was converted stoichiometrically to a monomeric form (M_r 110 000), and the monomeric form observed under nonreduced conditions (M_r 105 000) was converted to a heavy chain (M_r 60 000) and a light chain (M_r 50 000). The formation of a dimer of HMW kininogen was also confirmed by an immunoblotting experiment. This unique property of intact HMW kininogen to form a dimer was further utilized in studies on the kininogens and their derivatives as thiol proteinase inhibitors. The purified HMW kininogen strongly inhibited the caseinolytic activities of calpain I, calpain II, and papain but not those of trypsin, chymotrypsin, and thermolysin, indicating that it was a group-specific inhibitor for thiol proteinases. When HMW kininogen was reduced with 0.14 or 1.4 M β-mercaptoethanol, its inhibitory activity was partially or mostly inactivated, but on subsequent air oxidation its activity was almost completely recovered. In addition, kinin-free and fragment 1,2 free HMW kininogen showed higher inhibitory activity than the intact HMW kininogen. The heavy chain exhibited the highest activity and bound with 2 mol of papain per mole of the heavy chain. These results and the sequence data previously reported on low molecular weight (LMW) kininogen [Ohkubo, I., Kurachi, K., Takasawa, T., Shiokawa, H., & Sasaki, M. (1984) *Biochemistry 23*, 5691–5697] clearly demonstrated that two reactive sites for thiol proteinase inhibitor activity are located in the heavy chain of HMW and LMW kininogens and that the light chain and fragment 1,2 moieties of the kininogens interfere with the inhibitory activity of the heavy chain by steric hindrance.

High molecular weight (HMW)[1] kininogen has been reported to play two important physiological roles in liberating a vasoactive nonapeptide, bradykinin (Werle et al., 1948), and in functioning as a cofactor in the contact phase of the intrinsic blood coagulation cascade (Davie et al., 1975, 1979; Heimark et al., 1980). In the plasma, LMW kininogen, like HMW kininogen, is known to be a kinin precursor, but it does not accelerate coagulation, because it has no histidine-rich fragment (fragment 1,2) (Kato et al., 1981). HMW kininogen is composed of heavy and light chains held together with a disulfide bond, a bradykinin, and a histidine-rich fragment. On the other hand, LMW kininogen is composed of heavy and light chains linked by a disulfide bond and a bradykinin moiety. The bradykinin moieties and heavy chains of the two kininogens are identical, but their individual light chains are quite different in amino acid composition and size (Kitamura et al., 1983; Nawa et al., 1983).

† This work was supported in part by grants from the Ministry of Education, Science and Culture of Japan (Research Grant 60304094 to M.S. and Research Grant 59570519 to I.O.).
* Author to whom correspondence should be addressed.

[1] Abbreviations: HMW kininogen, high molecular weight kininogen; LMW kininogen, low molecular weight kininogen; TPI, thiol proteinase inhibitor; SDS, sodium dodecyl sulfate; PMSF, phenylmethanesulfonyl fluoride; Polybrene, hexadimethrine bromide; EDTA, ethylenediaminetetraacetic acid; Bz-L-Arg-pNA, *N*-benzoyl-L-arginine-*p*-nitroanilide; HRPO, horseradish peroxidase; SCM, reduced and S-carboxymethylated; β-ME, β-mercaptoethanol; Tris, tris(hydroxymethyl)-aminomethane; IgG, immunoglobulin G.

0006-2960/86/0425-1669$01.50/0